JOURNAL OF AGRICULTURAL AND FOOD CHEMISTRY

pubs.acs.org/JAFC Article

Proanthocyanidin Structural Details Revealed by Ultrahigh Resolution FT-ICR MALDI-Mass Spectrometry, $^{1}H-^{13}C$ HSQC NMR, and Thiolysis-HPLC–DAD

Savanah G. Reeves, Arpad Somogyi, Wayne E. Zeller, Theresa A. Ramelot, Kelly C. Wrighton, and Ann E. Hagerman*

Cite This: *J. Agric. Food Chem.* 2020, 68, 14038–14048 Read Online

ACCESS | Metrics & More | Article Recommendations | Supporting Information

ABSTRACT: Proanthocyanidins (condensed tannins) are important in food chemistry, agriculture, and health, driving demand for improvements in structure determination. We used ultrahigh resolution Fourier transform-ion cyclotron resonance mass spectrometry (FT-ICR MS) methods to determine the exact composition of individual species in heterogeneous mixtures of proanthocyanidin polymers from *Sorghum bicolor* grain and *Neptunia lutea* leaves. Fragmentation patterns obtained with FT-ICR ESI MS-MS (electrospray ionization) confirmed structural details from thiolysis-high-performance liquid chromatography (HPLC)–diode array detection (DAD) and $^{1}H-^{13}C$ heteronuclear single quantum coherence (HSQC) NMR. We found that A-type linkages were characteristic of shorter polymers in predominantly B-linked proanthocyanidin. We suggest that supramolecular complex formation between proanthocyanidins and matrix components such as 2,5-dihydroxybenzoic acid was responsible for anomalous 152 dalton peaks, incorrectly assigned as 3-*O*-galloylation, when using FT-ICR matrix-assisted laser desorption ionization (MALDI-MS). Our data illustrate the power of the ultrahigh resolution FT-ICR methods but include the caveat that MALDI-MS must be paired with complementary analytical tools to avoid artifacts.

KEYWORDS: *proanthocyanidin, tannin, supramolecular complex, dihydroxybenzoic acid, (epi)catechin gallate, (epi)gallocatechin gallate, $^{1}H-^{13}C$ HSQC NMR, FT-ICR, FT-IR*

INTRODUCTION

The plant natural products known as tannins are differentiated from other members of the polyphenol family by their ability to precipitate protein.[1] In common with other polyphenols, tannins are potent antioxidants and bind metals avidly.[2−4] Tannins are produced by most higher plants and are not only important to ecological processes[5] but also play roles in human and animal nutrition,[6,7] in food and beverage processing,[8,9] and in agricultural and industrial practices.[10,11] Given their ubiquitous occurrence and broad importance, it is not surprising that methods continue to be developed to qualitatively and quantitatively analyze tannins.[12−14]

Hydrolyzable tannins are derived from gallic acid; a core polyol such as glucose is esterified to gallic acid, with additional esterified or cross-linked galloyl groups to yield the ellagitannin moiety.[15] Hydrolyzable tannins can be isolated as single molecular species with a variety of chromatographic tools, and exact chemical structures of more than 1000 hydrolyzable tannins have been reported.[16,17] Condensed tannins, also known as proanthocyanidins, are oligomers and polymers of flavan-3-ol units with variations in hydroxylation patterns, *cis*- and *trans*-stereochemistry of C-ring substituents, position and nature of the interflavan bond (4 → 8 or 4 → 6, A- or B-type bonds), mean degree of polymerization (mDP), and degree of esterification (Figure 1).

In contrast to hydrolyzable tannins, it has been difficult to establish robust methods for elucidating the structural details of polymeric proanthocyanidins in part because isolation of individual molecular species is challenging.[18] In most studies, isolated fractions consisting of mixtures of polymers with different chain lengths and compositions are described in terms of bulk properties, often simply in terms of their subunit composition (procyanidin/prodelphinidin) and mDP. This information is generally obtained with a depolymerization technique such as thiolysis followed by high-performance liquid chromatography (HPLC) analysis.[19,20] Other methods that assess the intact proanthocyanidins include various mass spectrometric methods often in combination with HPLC. For example, HPLC coupled with electrospray ionization-mass spectrometry (ESI-MS) is useful for proanthocyanidin oligomers, but neither the chromatography nor the ionization work well for the larger polymers typically found in plant extracts.[21] Matrix-assisted laser desorption ionization-time of flight mass spectrometry (MALDI-TOF-MS) is now frequently used to confirm monomer composition and to provide supportive evidence for degree of polymerization, although the data can be limited by poor ionization of the higher-

Received: July 30, 2020
Revised: September 30, 2020
Accepted: October 29, 2020
Published: November 10, 2020

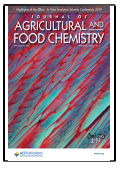

https://dx.doi.org/10.1021/acs.jafc.0c04877
J. Agric. Food Chem. 2020, 68, 14038–14048

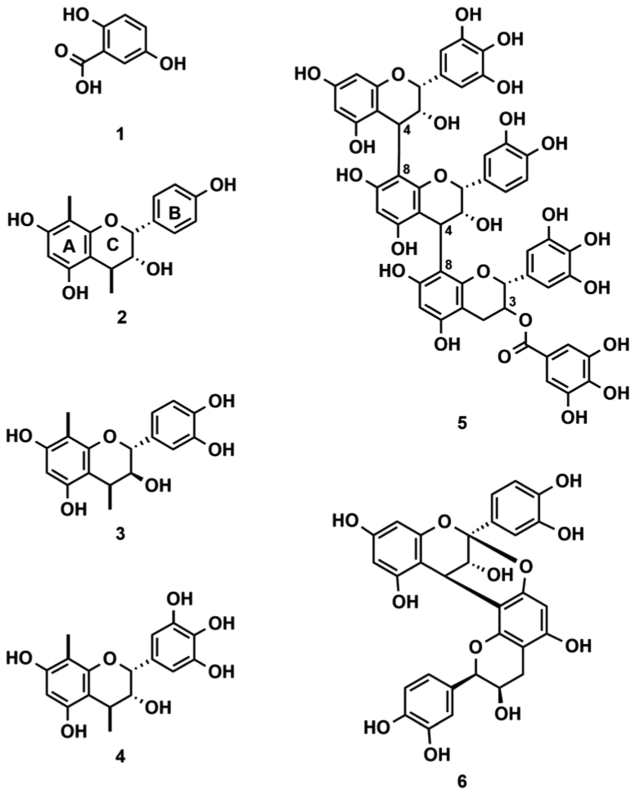

Figure 1. Structural formulae depicting the matrix 2,5-dihydroxybenzoic acid (DHB) and key features of proanthocyanidins. The matrix 2,5-dihydroxybenzoic acid (DHB) is a simple phenolic acid (**1**). In the proanthocyanidins, the B ring (**2**) can be substituted with 1, 2, or 3 phenolic groups yielding chain extender units classified as propelargonidin (**2**), procyanidin (**3**), and prodelphinidin (**4**). The stereochemistry on the C ring can be either trans (**3**) as in catechin or cis (**4**) as in epigallocatechin. The polymer is often esterified by gallic acid on the 3-hydroxyl of the C ring (**5**). Interflavan **4** → **8** C−C bonds between the A and C ring are most common (**5**), but the ether-containing A-type linkage (**6**) is typical of some plants.

molecular-weight species.[22] Other limitations of these widely employed methods include incomplete depolymerization during thiolysis, lack of commercial standards for the thiolysis products, and complex spectra arising from mixtures of cationized species in positive reflectron mode MALDI-TOF-MS.[23,24] NMR can reveal additional details, including presence of contaminating lipid or carbohydrate with simple proton NMR. $^{1}H-^{13}C$ heteronuclear single quantum coherence nuclear magnetic resonance (HSQC NMR) spectroscopy determines subunit composition and mDP, extent of galloylation, stereochemistry, and position of linkages between monomers,[25] but the method requires relatively large amounts of the sample and there is a significant barrier due to the expertise required to interpret the spectra.[26]

Ultrahigh resolution Fourier transform ion cyclotron resonance matrix-assisted laser desorption ionization mass spectrometry (FT-ICR MALDI-MS) has received limited attention as a tool to determine structural details and linkage types of proanthocyanidin molecules.[27,28] While thiolysis and NMR provide overall average structural information for the mixture of polymers in the typical heterogeneous samples, ultrahigh resolution FT-ICR MALDI-MS provides exact elemental composition of individual proanthocyanidin species in the mixtures. For example, the accurate mass measurement of the m/z 3025.55520 peak in the FT-ICR-MALDI-MS spectrum of the proanthocyanidin from *Neptunia lutea* resulted in a chemical composition of $C_{149}H_{117}O_{79}$ and the structure was assigned as [catechin, gallocatechin$_{(8)}$, gallate$_{(2)}$]$^{1-}$].[27]

We have recently noted that a significant shortcoming of MALDI-MS analysis of proanthocyanidins is the ambiguity of information about galloylation provided by the spectra. Galloylation is easily established with thiolysis or $^{1}H-^{13}C$ HSQC NMR, but MALDI-MS provides less useful data about gallate esters. Proanthocyanidins with gallate esters have characteristic clusters of peaks separated by 152.011 mass unit from the major flavan-3-ol polymer peaks, as expected for the addition of the $C_7H_4O_4$ gallate group.[27] However, the same peaks are found in MALDI-MS spectra from some proanthocyanidin samples that are not galloylated based on chemical or NMR data[29,30] (Figure 2). In this study, we used purified proanthocyanidin from *Sorghum bicolor* (L. Moench) grain, which is reported to be a simple procyanidin,[31] as a tool to examine more closely the basis for 152.011 mass differences in MALDI-MS data. Our goal was to provide insights that would ensure accurate interpretation of proanthocyanidin structures revealed by this powerful mass spectrometric method.

MATERIALS AND METHODS

Polyphenols. Mature grain from two genetically distinct lines of high tannin *S. bicolor* (L.) Moench was obtained and stored at 4 °C (Hi-Tannin Sumac NM03-9905, Scott Bean, USDA Manhattan Kansas and ICRISAT line IS8260, Gebisa Ejeta, Purdue University Department of Agronomy). Analysis was performed on at least two different preparations of proanthocyanidin from each variety of *Sorghum* for each of the techniques utilized.

Sorghum tannin was extracted from ground grain with methanol containing ascorbic acid and purified by ethyl acetate extraction to remove small phenolics, followed by Sephadex LH-20 chromatography to purify the high-molecular-weight fraction.[32,33] The freeze-dried powder was stored at −20 °C.

N. lutea proanthocyanidin was a gift from Harley Naumann, University of Missouri, Columbia, MO. Tannins were obtained from acetone−water extracts of the *Neptunia* leaf tissue followed by purification on a Sephadex LH20 column.[34]

Epigallocatechin gallate (EGCg) was a gift from Lipton Tea, Newark, NJ. Catechin, epicatechin, 2,5-dihydroxybenzoic acid (DHB), toluene-α-thiol, trifluoroacetic acid (TFA), and Sephadex LH-20 were obtained from Sigma Chemicals, St. Louis, MO, and used without further purification.

Thiolysis-HPLC−DAD. Purified proanthocyanidins were analyzed by thiolysis, according to published procedures.[19] Briefly, approximately 1 mg of proanthocyanidin was dissolved in 200 μL of methanol containing 30 μL of the HCl reagent (32% (v/v) HCl in methanol) and 72 μL of the thiol reagent (5% (v/v) toluene-α-thiol in methanol) and incubated at 40 °C for 30 min. The thiolytic degradation products were analyzed by HPLC using an Agilent 1100 HPLC with diode array detection and controlled by ChemStation Rev. A.09.03 software. The column was a Thermofisher Hypersil Gold C8 (160 × 4.6 mm, 3 μm). Sample injection volume was 10 μL. The gradient program employed 0.13% (v/v) trifluoroacetic acid (TFA) in nanopure water (A) and 0.10% (v/v) TFA in acetonitrile (B) at a flow rate of 0.5 mL/min at 27.0 °C for a 48 min duration, as follows: 0−3 min, isocratic at 15% B; 3−8 min, increase to 20% B; 8−10 min, increase to 30% B and hold isocratic until 28 min; 28−32 min, increase to 70% B; 37−40 min, decrease to 15% B, and re-equilibrate.[19] Reaction products were detected at 220 nm and were identified by their retention times and spectral characteristics compared to authentic standards.[19,20] Products were quantitated based on peak areas and converted to moles of extender and terminal units. The chromatograms from control samples that did not contain

https://dx.doi.org/10.1021/acs.jafc.0c04877
J. Agric. Food Chem. 2020, 68, 14038−14048

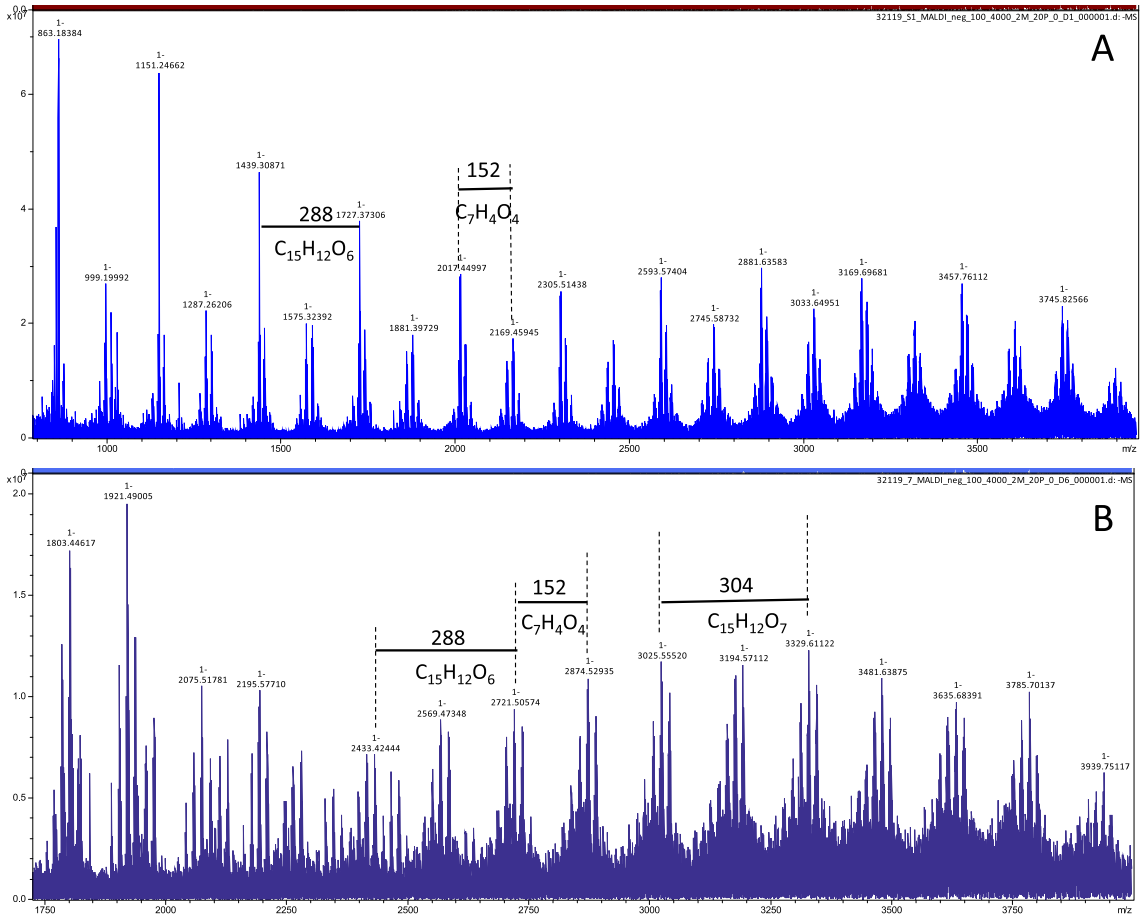

Figure 2. Ultrahigh resolution FT-ICR MALDI-MS spectra in the negative ion mode obtained with proanthocyanidin from *S. bicolor* var. Sumac grain (A) and *N. lutea* leaves (B). The matrix was 2,5-dihydroxybenzoic acid.

acid or thiol and were not heated were used to confirm that all of the proanthocyanidin was degraded by thiolysis and to confirm that the proanthocyanidin did not contain any flavan-3-ol monomer contamination that would interfere with terminal unit determination.

NMR. ^{1}H, ^{13}C, and $^{1}H-^{13}C$ HSQC NMR spectra were recorded at 27 °C on a BrukerBiospin DMX-500 (^{1}H 500.13 MHz, ^{13}C 125.76 MHz) instrument equipped with TopSpin 3.5 software and a cryogenically cooled 5 mm TXI $^{1}H/^{13}C/^{15}N$ gradient probe in inverse geometry. Spectra were recorded in DMSO-d_6 and were referenced to the residual signals of DMSO-d_6 (2.49 ppm for ^{1}H and 39.5 ppm for ^{13}C spectra). ^{13}C NMR spectra were obtained using 1K scans (acquisition time 56 min). For $^{1}H-^{13}C$ HSQC experiments, spectra were obtained between 200 and 620 scans (depending on sample size and instrument availability) obtained using the standard Bruker pulse program (hsqcetgpsisp.2) with the following parameters: Acquisition: TD 1024 (F2), 256 (F1); SW 16.0 ppm (F2), 165 ppm (F1); O1 2350.61 Hz; O2 9431.83 Hz; D1 = 1.50 s; CNST2 = 145. Acquisition time: F2 channel, 64 ms, F1 channel 6.17 ms. Processing: SI =1024 (F2, F1), WDW = QSINE, LB = 1.00 Hz (F2), 0.30 Hz (F1); PH_mod = pk; Baseline correction ABSG = 5 (F2, F1), BCFW = 1.00 ppm, BC_mod = quad (F2), no (F1); Linear prediction = no (F2), LPfr (F1). Sample sizes used for these spectra ranged from 5 to 10 mg providing NMR sample solutions with concentrations of 10–20 mg/mL.

Ultrahigh Resolution FT-ICR MALDI-MS, Negative Ion Mode. Solutions of purified proanthocyanidin samples were prepared (15 mg/mL) using reagent grade methanol and 1 μL was then mixed with 10 μL of saturated DHB matrix solution (ca. 0.1 M in acetonitrile:water, 1:1, containing 0.1% formic acid). A 1 μL aliquot of this sample–analyte mixture was deposited on a conventional stainless steel MALDI plate and allowed to dry before inserting into the Bruker 15T SolariX XR FT-ICR MALDI-MS (Bruker Daltronics GmbH, Bremen, Germany). External calibration was run on a standard peptide mix (Bruker Daltonics, Billerica, MA) in the negative ion mode, while a more accurate internal calibration was performed using DHB cluster peaks. Typically, 20% of the YAG/Nd (351 nm) laser power was used for the spectral acquisition and 100 scans were accumulated. The FT-ICR mass resolution was set to about 400 000.

FT-ICR ESI-MS, Negative Ion Mode. Ultrahigh resolution mass spectra were acquired on a Bruker SolariX XR FT-ICR MS (Bruker Daltronics GmbH, Bremen, Germany) equipped with a 15 Tesla superconducting magnet (Magnex Scientific Inc., Yarnton, GB) and an Apollo II ESI source (Bruker Daltonics GmbH, Bremen, Germany) operated in the negative ionization mode. (Note that the SolariX XR instrument has a double ionization source used for both the MALDI and the ESI instruments). Negative ionization has already been proven to be the preferred ionization mode in fingerprinting wines by FT-ICR MS[35] and, more recently, humic acid derivatives.[36] Proanthocyanidin samples were dissolved in acetonitrile:water 1:1 solvent mixture in a concentration range of 3–5 μM. These solutions were then introduced by direct infusion into the electrospray source at a flow rate of 120 μL/h. FT-ICR-MS was externally calibrated using an Agilent calibration standard (Agilent Technologies, Santa Clara, CA) diluted 10-fold with acetonitrile:water 1:1. Some well-known background ions (generated e.g., from alkylbenzene sulfonate detergents) were also used for calibration of the lower m/z range. The mass resolution was set to about 400 000 and the mass accuracy was <2 ppm.

Methanolysis/HPLC. Equal volumes of 2 mg/mL proanthocyanidiin in methanol and 1 M HCl in methanol were mixed, evacuated to remove oxygen, and incubated at 70 °C for 24 h. The methanolized samples and controls without HCl were diluted 10-fold with MeOH

https://dx.doi.org/10.1021/acs.jafc.0c04877
J. Agric. Food Chem. 2020, 68, 14038–14048

Table 1. FT-ICR MALDI-MS Data for Proanthocyanidin from *S. bicolor* var. Sumac and *N. lutea*[a]

peak (m/z)	calculated mass (m/z)	error (ppm)	m/z +288[b]	m/z +304[c]	m/z +152[d]	# A-type linkages	apparent composition[e]
			S. bicolor				
863.1838	863.1823	1.73	3	0	0	1	cat_3
1015.1946	1015.1933	1.32	3	0	1	1	cat_3 g
1151.2466	1151.2457	0.77	4	0	0	1	cat_4
1303.2591	1303.2567	1.83	4	0	1	1	cat_4 g
1439.3087	1439.3091	0.29	5	0	0	1	cat_5
1591.3218	1591.3200	1.07	5	0	1	1	cat_5 g
1727.3731	1727.3725	0.32	6	0	0	1	cat_6
1881.3973	1881.3991	0.98	6	0	1	0	cat_6 g
2017.4456	2017.4515	2.98	7	0	0	0	cat_7
2169.4595	2169.4625	1.41	7	0	1	0	cat_7 g
2305.5144	2305.5149	0.25	8	0	0	0	cat_8
2457.5217	2457.5259	1.71	8	0	1	0	cat_8 g
2593.5740	2593.5783	1.66	9	0	0	0	cat_9
2745.5873	2745.5893	0.72	9	0	1	0	cat_9 g
2881.6502	2881.6417	2.94	10	0	0	0	cat_{10}
3033.6495	3033.6527	1.05	10	0	1	0	cat_{10} g
			N. lutea				
911.1681	911.1671	1.11	0	3	0	1	$gallocat_3$
1047.1845	1047.1831	1.36	1	2	1	1	$cat_1gallocat_2$ g
1063.1793	1063.1780	1.22	0	3	1	1	$gallocat_3$ g
1199.1963	1199.1941	1.84	1	2	2	1	cat_1 $gallocat_2$ g_2
1217.2065	1217.2046	1.55	0	3	2	0	$gallocat_3$ g_2
3025.5552	3025.5596	1.45	1	8	2	0	$cat_1gallocat_8$ g_2

[a]The samples were mixed with the matrix, 2,5-dihydroxybenzoic acid (DHB), before spotting on the plate and obtaining the high-resolution spectra. [b]Mass unit value 288 dalton represents the number of (epi)catechin subunits. [c]Mass unit value 304 dalton represents the number of (epi)gallocatechin subunits. [d]Mass unit value 152 dalton represents the number of apparent galloyl ester groups. [e]Abbreviations (epi)catechin (cat), (epi)gallocatechin (gallocat), and 3-*O*-gallate ester (g). The reported gallate ester values ignore the contribution of supramolecular complexes with the matrix, DHB.

before injecting 10 μL on the HPLC system described above. The gradient utilized 0.13% (v/v) trifluoroacetic acid in water (A) and 0.10% (v/v) TFA in acetonitrile (B) at a flow rate of 0.5 mL/min at 27 °C for a duration of 40 min, as follows: 0−4 min, 2% B; 4−8 min, increase to 20% B; 8−10 min, increase to 30% B and hold isocratic until 30 min; 30−35 min, increase to 70% B; 40−41 min return to 2% B followed by re-equilibration. Reaction products were detected at 220 nm and were identified by their retention times and spectral characteristics, as compared to authentic standards. Commercial methyl gallate (>99.5%) was used to determine that the lower limit of detection was 0.3% galloylation or less than 1 gallate ester group per 100 flavan-3-ol subunits in the proanthcyanidin.

Fourier Transform Infrared Spectroscopy. Infrared spectra were collected with a Harrick SplitPea ATR microscope interfaced to a PerkinElmer Spectrum 100 Fourier transform infrared spectrometer. This accessory employed a germanium internal reflection element (IRE) and the standard deuterium triglycine sulfate (DTGS) detector on the Spectrum 100 macro bench. Spectra collected using this device represent the average of 32 individual scans possessing a spectral resolution of 4 cm^{-1}. About 1−2 mg of each sample was pressed into a pellet and was brought into intimate contact with the IRE using a loading of 0.5 kg.

NMR of Matrix-Proanthocyanidin Mixtures (Complexation). ^{1}H NMR spectra were recorded at 298 K on a Bruker AV500, equipped with a Topspin, 5 mm BBO probe with Z-gradients. Spectra were recorded in D_2O, using water suppression on the solvent signal at 4.8 ppm, and were obtained using a one-dimensional nuclear Overhauser effect spectroscopy (1D NOESY) method (10 ms mixing time) with 8−16 scans (acquisition time less than 2 min). Solutions were prepared by dissolving 4 mg of proanthcyanidin or matrix in 5 mL of D_2O and diluting the matrix solution 1:1 with tannin solution or D_2O.

RESULTS AND DISCUSSION

MALDI-MS provides insights into proanthocyanidin structure by revealing overall composition of the tannin, although the amounts of higher-molecular-weight species are underestimated due to inefficient ionization. By using high-resolution FT-ICR-MALDI-MS, the exact subunit composition of individual chemical species that comprise purified proanthocyanidin mixtures can be established.[27] The overall composition can be established by examining the intervals between clusters of peaks in either MALDI-TOF or FT-ICR-MALDI-MS spectra. The intervals between the major clusters of peaks correspond to the flavan-3-ol subunits, for example, (epi)-catehin (288 dalton difference) or (epi)gallocatechin (304 dalton difference) (Figure 2).[26] Intervals between minor peaks reveal modifications on the polymer such as the relatively common addition of a gallate ester at position 3 on the C-ring of the parent subunit (152 dalton difference) (Figures 1 and 2). With high-resolution data, details of the structure can be extracted by matching subunit composition and modifications including galloylation to the accurate masses corresponding to individual peaks in the spectrum. The molecular weight resolution is sufficient to easily identify and quantify structural variations such as A-type linkages (−2.01565, corresponding to 2 hydrogens),[28,37] and theoretical isotopic distribution patterns can be modeled to confirm structural identifications (Supporting Information, Figure S1).

When assessing various preparations with FT-ICR MALDI MS, we were surprised to find the mass difference of 152 dalton between peaks in the spectra of proanthocyanidins that are reported not to contain gallate esters, including

https://dx.doi.org/10.1021/acs.jafc.0c04877
J. Agric. Food Chem. 2020, 68, 14038−14048

Table 2. Thiolysis-HPLC−DAD and $^{1}H-^{13}C$ HSQC NMR Structural Data for Condensed Tannin from *S. bicolor* var. IS8661 and *N. lutea*[a]

	mDP		% *cis*		% PD		% gallate		% A-type
plant	thiolysis	NMR	thiolysis	NMR	thiolysis	NMR	thiolysis	NMR	NMR
Sorghum	16.3	16.6	91.2	90.4	4.0	0	0	0	5.3
Lutea	11.5	8.1	93.0	91.5	88.0	91.8	32.0	34.4	0

[a]Peak areas from thiolysis and integrated areas of $^{1}H-^{13}C$ HSQC NMR cross peaks were used to calculate mean degree of polymerization (mDP), epicatechin composition (% *cis*), tri- vs dihydroxylation on the B ring (% prodelphinidin), % 3-*O*-gallate esters, and A-type linkages.

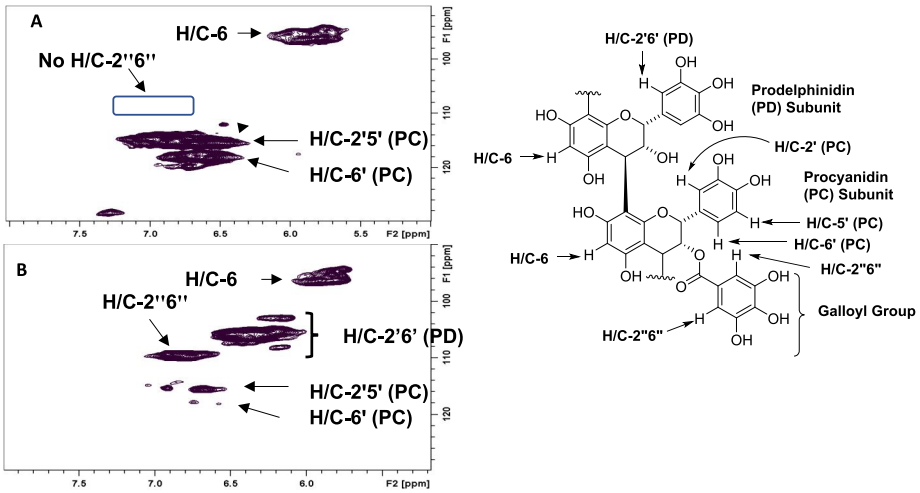

Figure 3. Expanded aromatic regions from the $^{1}H-^{13}C$ HSQC NMR spectra of purified proanthocyanidins from *S. bicolor* (A) and *N. lutea* leaves (B). The relevant two-dimensional (2D) NMR cross-peaks are labeled. Note that the NMR cross-peak signal for H/C-2″6″ of the the galloyl group is not evident in the Sorghum tannin sample.

procyanidin from *Sorghum* grain (Figure 2).[23,31] The data suggested that each of the proanthocyanidin species (trimer, tetramer, etc.) exists as both an ungalloylated oligomer and as a monogallate (Table 1), implying that the 16-mer *Sorghum* tannin could be about 5% 3-*O*-galloylated. To establish the basis for these 152 mass differences, we did a detailed analysis of the proanthocyanidin from *Sorghum* grain. Proanthocyanidin from *N. lutea* served as a model compound for galloylated tannin.[27] Samples of epigallocatechin gallate and catechin acted as galloylated and ungalloylated monomeric controls, respectively.

We evaluated the composition and especially the degree of galloylation of the two proanthocyanidins with chemical and spectroscopic methods. Based on previous reports, thiolysis indicated that *Sorghum* proanthocyanidin was mainly comprised of epicatechin and contained little to no (epi)-gallocatechin, in contrast to the *Neptunia* tannin, which was 88% epigallocatechin (Table 2). Most importantly, the thiolysis confirmed previous reports that *Sorghum* proanthocyanidin did not contain gallate esters[31,38] but that *Neptunia* proanthocyanidin is highly galloylated (Table 2).[27]

$^{1}H-^{13}C$ HSQC NMR establishes the interflavan bonding pattern as well as the composition of proanthocyanidins, as described in detail in earlier publications.[25,39] Cross peaks centered around (4.4, 36) ppm and (4.4, 38) ppm were identified as H/C-4 signals corresponding to epi(gallo)-catechin and (gallo)catechin flavan-3-ol subunits, respectively. Based on the ratio of the areas, the compositions established by thiolysis were confirmed, with *Sorghum* proanthocyanidin predominantly based on epicatechin and *Neptunia* proanthocyanidin on epigallocatechin subunits (Table 2). Unlike thiolysis, NMR provides direct evidence for interflavan bonding patterns, with cross peaks centered at (4.4, 36/38) ppm and (4.3, 29) ppm characteristic of B-type linkages and A-type linkages, respectively. Based on the relative peak areas, it was determined that the *Sorghum* proanthocyanidin contained 5.3% A-type linkages, while the *Neptunia* proanthocyanidin was 100% B-type linkages (Table 2). Most relevant for our analysis were the cross peaks for the 2″, 6″ C−H bonds (6.8, 110 ppm) of the galloyl group that indicate the presence of gallate esters. The $^{1}H-^{13}C$ HSQC NMR spectrum of *Sorghum* did not provide any evidence for galloylation, while the *Neptunia* proanthocyanidin contained 34.4% 3-*O*-gallate esters, consistent with the thiolysis data (Table 2 and Figure 3).

Infrared (IR) spectra provided additional support for the conclusion that the *Sorghum* proanthocyanidin did not contain gallate groups despite the evidence from the FT-ICR-MALDI-MS. The Fourier Transform IR spectrum of epigallocatechin gallate, a simple flavan-3-ol gallate ester, displays a characteristic ester carbonyl peak at 1690 cm^{-1}, while the IR spectrum of catechin, the ungalloylated flavan-3-ol, did not exhibit an ester band (Figure 4). Consistent with our other analyses, the spectrum of *Neptunia* proanthocyanidin possessed an ester band but the *Sorghum* proanthocyanidin spectrum did not have any peaks in this region (Figure 4).

We established methanolysis reaction conditions for releasing methyl gallate from esterified proanthocyanidins with a limit of detection of 0.3% galloylation or less than one gallate group per 100 subunits. No detectable methyl gallate was released from *Sorghum* proanthocyanidin under these conditions, but methyl gallate was a dominant peak in the products from the *Neptunia* proanthocyanidin methanolysis reaction (Supporting Information, Figure S2).

https://dx.doi.org/10.1021/acs.jafc.0c04877
J. Agric. Food Chem. 2020, 68, 14038−14048

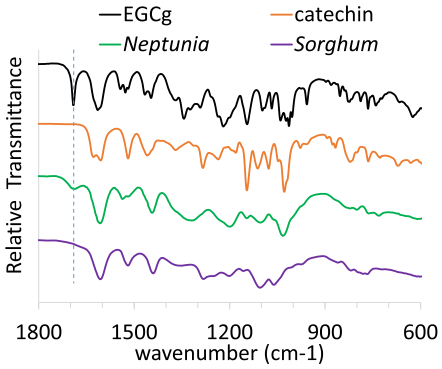

Figure 4. FTIR spectra of epigallocatechin gallate (black), catechin (orange), *N. lutea* proanthocyanidin (green), and *S. bicolor* var. IS8260 proanthocyanidin (purple). The characteristic ester band (1690 cm^{-1}) is indicated with a dotted blue line.

We carried out negative ion FT-ICR ESI-MS measurements as an alternative mass spectrometric method that is distinct from MALDI-MS because it does not require the small-molecule matrix and because it promotes fragmentation that facilitates identification of specific ions. Positive ion mode spectra of the samples had complex patterns of associated ion complexes (sodium, potassium, or ammonium) but the patterns in negative mode corresponded to the expected series of peak clusters separated by 288 dalton ($C_{15}H_{12}O_6$) for *Sorghum* proanthocyanidin. The series of apparent gallate esters noted in the MALDI spectra (e.g., *m/z* 1015, *m/z* 1303 etc.) were not detected in the FT-ICR-MS spectra. Peaks with −2 charge were common, with −1 and −3 charged peaks also populating the spectra. There were no intervals corresponding to (epi)catechin gallate (440 dalton) or (epi)gallocatechin gallate (456 dalton), confirming that the *Sorghum* proanthocyanidin does not have galloyl esters.

Peaks with multiple charges generally give more characteristic fragments, so we did tandem MS/MS analysis with gas phase collisional induced dissociation (CID) on the ion at *m/z* 864.19078, identified as $[(epi)catechin]_{(6)}^{2-}$ ($C_{90}H_{72}O_{36}$, Table 3). The main fragments clearly correspond to quinone methide (QM) fission with losses of 288 ($C_{15}H_{12}O_6$), see e.g., ions at *m/z* 287, 289, 575, 577, 863, 865, and 1151 (Figure 5 and Table 3).[22] This pattern of fragmentation indicates predominantly B-type interflavan linkages. Fragments characteristic of heterocyclic ring fission (HRF) were detected (Figure 5 and Table 3) but there was no evidence for reverse Diels−Alder fragmentation (RDA).[26] Galloylated proanthocyanidins yield fragments corresponding to loss of 169 dalton in ESI-MS, due to cleavage of the ester bond and release of gallic acid ($C_7H_5O_5^{1-}$),[40] but this product was not found in our *Sorghum* MS-MS spectra. Note that due to low signal intensity a relatively wide window (Δm = 5) was used for ion selection, thus some ions with low intensities at around the selected *m/z* 864 ion may result in some low-intensity fragments, identified by comparison of the parent ion spectrum to the theoretical isotope pattern (Supporting Information, Figure S1). The appearance of these fragments does not influence the main conclusion that almost exclusively B-type fragments are observed with a mass difference of 288 dalton. Overall, the MS-MS data are consistent with the other data on *Sorghum* obtained by chemical and spectroscopic methods described here and support the conclusion that gallate esters do not comprise structural elements in this proanthocyanidin.

To better understand the anomalous 152.011 dalton mass differences in the FT-ICR-MALDI data, we re-examined the MALDI spectra in more detail. We were able to identify *Sorghum* proanthocyanidin polymers consisting of (epi)-catechin subunits with degrees of polymerization up to 13 (Table 1). The apparent discrepancy between this polymer distribution and the mDP 16 established by thiolysis and NMR is a consequence of the inefficient ionization of higher-molecular-weight species in MALDI experiments.[41] Higher polymers are under-represented in the MALDI-MS and the method cannot be used to establish accurate mDP. Peaks were also assigned as species containing A-type linkages (Table 1), consistent with our other chemical and spectroscopic data.

A unique feature of the ultrahigh-resolution FT-ICR MALDI is the ability to assign structural feature such as linkage type to individual molecular species. For example, this data revealed that in *Sorghum* proanthocyanidin, A-type linkages were more common in shorter oligomers, with degrees of polymerization

Table 3. FT-ICR ESI-MS/MS Data of the (Epi)catechin$_6$ (*m/z* 864.190713^{2-}) Species in Condensed Tannin from *S. bicolor* var. 8661[a]

m/z measured	*m/z* calculated	formula	error (ppm)	assignment	cleavage type
864.19078	864.190713	$[(C_{15}H_{12}O_6)_6H_2 - 2H]^{2-}$	0.08	$[M - 2H]^{2-}$	parent ion (hexamer) (−2)
1151.2461	1151.24627	$[(C_{15}H_{12}O_6)_4 - H]^-$	0.15	$[M - 2H - 2C_{15}H_{12}O_6]^-$	QM
865.19841	865.198538	$[(C_{15}H_{12}O_6)_3 + H]^-$	0.15	$[M - 2H - 3C_{15}H_{12}O_6 + H]^-$	QM
863.18232	863.182888	$[(C_{15}H_{12}O_6)_3 - H]^-$	0.66	$[M - 2H - 3C_{15}H_{12}O_6 - H]^-$	QM
739.16632	739.166844	$[(C_{15}H_{12}O_6)_2 + C_9H_6O_3 + H]^-$	0.71	$[M - 2H - 3C_{15}H_{12}O_6 - C_6H_5O_3 + H]^-$	HRF
737.15074	737.151194	$[(C_{15}H_{12}O_6)_2 + C_9H_6O_3 - H]^-$	0.62	$[M - 2H - 3C_{15}H_{12}O_6 - C_6H_5O_3 - H]^-$	HRF
701.15123	701.151194	$C_{36}H_{29}O_{15}$	0.05		unassigned
695.13974	695.140629	$C_{37}H_{27}O_{14}$	1.37		unassigned
693.12408	693.124979	$C_{37}H_{25}O_{14}$	1.30		unassigned
577.13477	577.135150	$[(C_{15}H_{12}O_6)_2 + H]^-$	0.66		QM
575.11911	575.119500	$[(C_{15}H_{12}O_6)_2 - H]^-$	0.68		QM
451.10320	451.103456	$[C_{15}H_{12}O_6 + C_9H_6O_3 + H]^-$	0.57	$[M - 2H - 4C_{15}H_{12}O_6 - C_6H_5O_3 + H]^-$	HRF
449.08740	449.087806	$[C_{15}H_{12}O_6 + C_9H_6O_3 - H]^-$	0.90	$[M - 2H - 4C_{15}H_{12}O_6 - C_6H_5O_3\text{-}H]^-$	HRF
289.07122	289.071762	$[C_{15}H_{12}O_6 + H]^-$	1.87	monomer	QM
287.05601	287.056112	$[C_{15}H_{12}O_6 - H]^-$	0.36	monomer	QM

[a]The MS/MS products are formed by quinone methide (QM) fission and heterocyclic ring fission (HRF). The spectrum is provided in Figure 5, and details of the fragmentation pathways for proanthocyanidins with B- and A-type linkages are summarized in ref 25.

https://dx.doi.org/10.1021/acs.jafc.0c04877
J. Agric. Food Chem. 2020, 68, 14038−14048

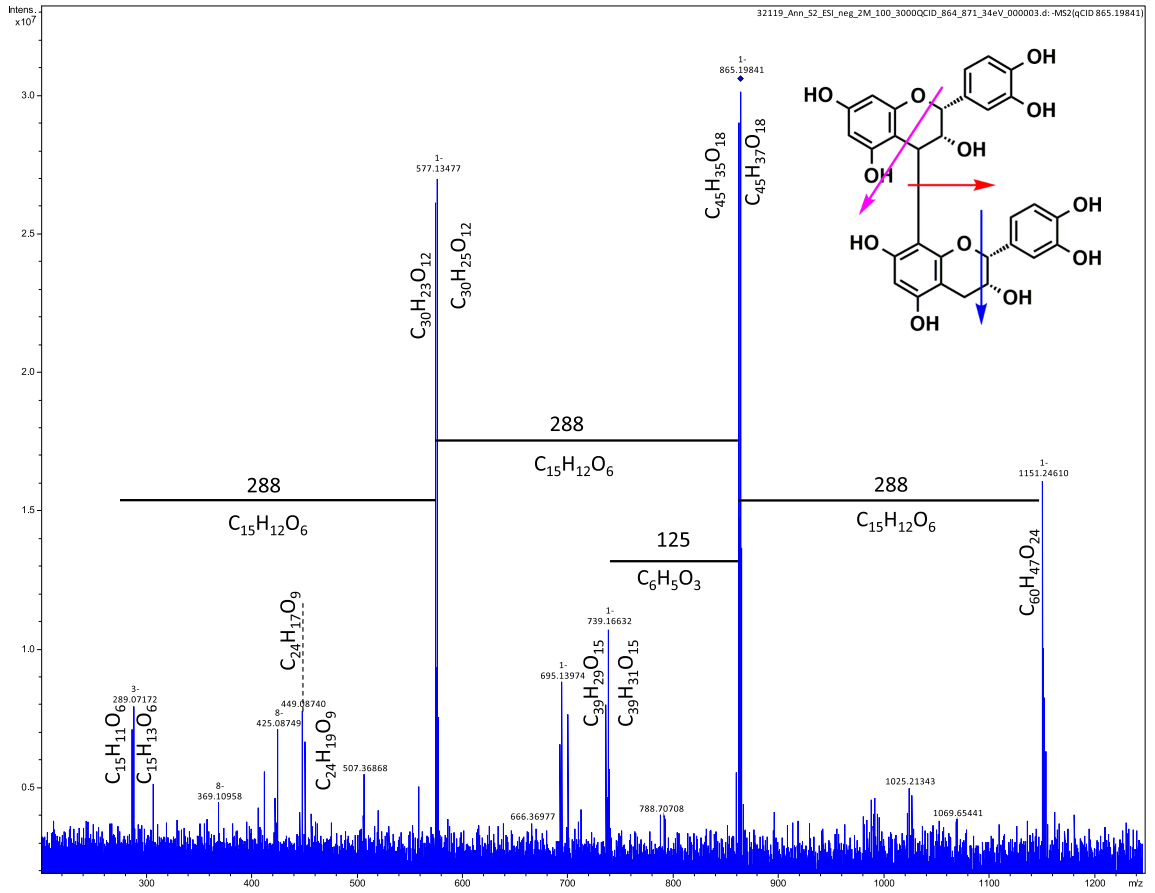

Figure 5. FT-ICR ESI MS/MS of *S. bicolor* var. IS8260 proanthocyanidin. The molecular ion *m/z* 864.190782- ($C_{90}H_{72}O_{36}$) is the hexamer of (epi)catechin. The inset shows the typical fragmentation pattern for a proanthocyanidin illustrated for a dimer.[26] Quinone methide (QM) interflavan bond cleavage (red line) releases the upper unit as catechin ($C_{15}H_{13}O_6^{1-}$, 289 Da) and the lower unit as the quinone ($C_{15}H_{11}O_6^{1-}$, 287 Da). Heterocyclic ring fission (HRF, pink line) releases phloroglucinol ($C_6H_5O_3^{1-}$, 125 Da) and rearranges the residual flavonol fragment ($C_9H_6O_3^{1-}$, 162 Da). Reverse Diels–Alder (RDA) reactions (blue line) release $C_8H_7O_3^{1-}$ (151 Da) and rearrange the residual fragment ($C_7H_5O_3^{1-}$, 137 Da). A comprehensive fragment list is provided in Table 3.

from 3 to 6, and less common in the more highly polymerized species (Table 1). A similar pattern was revealed in a structural survey of proanthocyanidins from a wide range of fruits, with A-type linkages more prevalent in tetramer–heptamers and less abundant in octamers and larger oligomers,[42] although in peanuts the percentage of A-type linkages was higher in octamers than in smaller oligomers.[43] It has been suggested that A-type linkages are formed through oxidation of B-linked proanthocyanidins either by polyphenol oxidase or laccase[44,45] or by free radical mechanisms.[46] The preferential distribution of A-type linkages in shorter polymers may provide indirect support for the enzymatic mechanism if there is a substrate size limitation to the oxidizing activity of participating enzymes. An alternative hypothesis is that addition of A-type linkages during the normal polymerization process may halt further polymerization of the proanthocyanidin, preventing extension to longer polymers. Additional research into factors dictating the number and positions of A-type linkages in proanthocyanidin is warranted based on the many studies suggesting unique bioactivity for A-linked proanthocyanidins.[47]

More detailed analysis of the FT-ICR MALDI-MS data obtained with *Neptunia* tannin showed that this proanthocyanidin existed in multiple galloylated forms including mono-, di-, and triesterified polymers (Table 1). Similar highly galloylated proanthocyanidins have been reported in *Rumex*, such as procyanidin dimers, trimers, and tetramers esterified with two gallates (e.g., dimer B2 digallate).[48] The variation in galloylation implies a high level of heterogeneity in the *Neptunia* proanthocyanidin but is consistent with the average assessment of about 33% gallate ester from thiolysis and NMR studies (Table 2). The simplest interpretation of the FT-ICR MALDI-MS data for the *Sorghum* proanthocyanidin was that each species consisted of an ungalloylated form and a monogallate (Table 1), but this was inconsistent with all our other chemical and spectroscopic data.

All of our other methods of analysis supported the conclusion that *Sorghum* proanthocyanidin does not contain gallate ester groups. The peaks with intervals of 152 dalton ($C_7H_4O_4$) in the FT-ICR MALDI-MS appear to be an unreliable indicator of galloylation of proanthocyanidins. Even the ultrahigh-resolution data do not discriminate between galloylated proanthocyanidins (e.g., *Neptunia*) and ungalloylated forms (e.g., *Sorghum*). We postulated that the intervals of 152 dalton are an artifact of the DHB matrix employed in MALDI-MS and the strong binding properties of proanthocyanidins.[49]

Supramolecular structures are complexes that form due to strong noncovalent interactions between molecules, including forces such as ion pairing, electrostatic interactions, ion–π interactions, hydrogen bonding, solvophobic interactions,

https://dx.doi.org/10.1021/acs.jafc.0c04877
J. Agric. Food Chem. 2020, 68, 14038–14048

dispersive interactions, and stacking interactions.[50] Formation of supramolecular complexes via $\pi-\pi$ stacking is characteristic of polyphenols including flavonoids, hydrolyzable tannins, and phenolic acids. For example, co-pigmentation, the well-known phenomenon that dictates the hue, intensity, and stability of color, for example, in wines and ornamental flowers, results from supramolecular complex formation between an anthocyanin pigment and one or more other phenolic compounds.[51] Although proanthocyanidins appear to bind only weakly to anthocyanins,[52,53] formation of supramolecular complexes between proanthocyanidins and proteins or other biomolecules has been exploited to create materials with unique properties.[54]

We used ^{1}H NMR to evaluate whether proanthocyanidins form supramolecular complexes with 2,5-dihydroxybenzoic acid (DHB, Figure 1), the matrix that we employed to facilitate ionization in the FT-ICR MALDI-MS experiments. Supramolecular complexes involving $\pi-\pi$ stacking interactions can be detected by an upfield shift in the resonances of the aromatic protons due to increased shielding in the complex.[51] The ^{1}H NMR spectrum of DHB had three doublets at 7.24 ppm, 6.95 ppm, and 6.79 ppm that were shifted upfield, δ 0.026 to 0.049 ppm, when the DHB was mixed with *Sorghum* proanthocyanidin (Figure 6). A similar upfield shift was

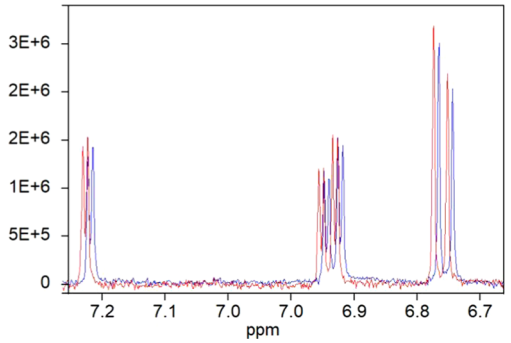

Figure 6. ^{1}H NMR spectra of DHB (red) and of the mixture of DHB plus *S. bicolor* var. IS8661 proanthocyanidin (blue) in D_2O.

observed with mixtures of DHB and *Neptunia* proanthcyanidin, leading us to conclude that galloylated proanthocyanidins also complexed the phenolic acid (Supporting Information, Figure S3). Complexation of small aromatic molecules by ungalloylated and galloylated proanthocyanidins follows the precedent established in studies of flavan-3-ol gallates and flavan-3-ols with caffeine, a flat aromatic molecule that forms strong complexes with phenolics.[49]

We propose that a strong supramolecular complex is formed by the insertion of DHB between the aromatic rings of the flavan-3-ol subunits of the proanthocyanidins. Our data suggest that the complexes are stable during the "soft" ionization process of MALDI, so that the spectra include discrete mass peaks for the proanthocyanidin itself [M$^-$] and for its DHB complexes [M$^-$ (+) DHB$^-$]. This model is supported by previous studies in which an interval of 152.26 dalton was identified as an oligosaccharide−DHB supramolecular complex stabilized by hydrogen bonds between the deprotonated saccharide alcohol and deprotonated DHB carboxylate.[55] For the proanthocyanidins, the deprotonated DHB and the gallate ester have identical molecular formulas ($C_7H_5O_4$). The proposed supramolecular complexes comprising deprotonated proanthocyanidin plus deprotonated DBH are indistinguishable from deprotonated proanthocyanidin 3-*O*-gallates even with ultrahigh-resolution FT-ICR MALDI-MS. For ungalloylated proanthocyanidins, the DHB-related peaks would be incorrectly attributed to galloyl esters, while for galloylated proanthocyanidins, association with DHB could lead to overestimation of the degree of esterification.

Many other matrices are available for MALDI-MS, but we and others have found that DHB typically provides the best ionization and the best-quality spectra with proanthocyanidin samples.[29] For example, dithranol, α-cyano hydroxycinnaic acid (HCA), and sinapinic acid (SA) gave much lower-quality spectra than DHB in our hands, consistent with the literature.[56] We used ^{1}H NMR to assess complex formation with SA to evaluate if this class of compounds could provide noninteracting matrices. In this case, we observed a downfield shift (δ −0.007 to −0.015 ppm) in the aromatic proton signals when the Sorghum proanthocyanidin was added to the SA (Supporting Information, Figure S4). The hydroxycinnamic acids have a short unsaturated side chain that must alter interaction with proanthocyanidin so that the aromatic protons are deshielded in the complex compared to the shielding that takes place when the proanthocyanidin binds a benzoic acid.[57]

In addition to highlighting the need to find better matrices to fully realize the potential of ultrahigh-resolution FT-ICR MALDI-MS, our study re-emphasizes the importance of using more than one analytical technique to obtain structural information about complex natural products such as proanthocyanidins. In particular, we note that different ionization techniques can reveal different components of complex mixtures.[36] Finally, MALDI-MS has received little attention as a method for analyzing hydrolyzable tannins, because these compounds are amenable to purification to single species that can be identified with routine HPLC-MS analysis. Attempts to employ MALDI-MS for hydrolyzable tannins and other polyphenols[58] should address the potential for matrix effects given the strong tendency of gallate groups to bind small aromatic molecules.[49]

■ ASSOCIATED CONTENT

Supporting Information

The Supporting Information is available free of charge at https://pubs.acs.org/doi/10.1021/acs.jafc.0c04877.

FT-ICR-ESI-MS for *S. bicolor* var. 8661 tannin. Inset table shows calculated *m*/*z* values for the isotopomers of the parent ion, $C_{90}H_{72}O_{36}$, [(epi)catechin]$_{(6)}^{2-}$ (Figure S1); HPLC data from typical methanolysis analysis; samples of *N. lutea* proanthocyanidin or *S. bicolor* proanthocyanidin were methanolized to release gallate esters as methyl gallate; the products were separated by RP-HPLC with detection at 220 nm; products include anthocyanidins produced from the flavan-3-ol monomers of the proanthocyanidin in addition to methyl gallate from *Neptunia* (green) but not from *Sorghum* (purple); the methyl gallate standard (gray) elutes at 15.1 min (Figure S2); ^{1}H NMR spectra of 2,5-dihydroxybenzoic acid (red) and of the mixture of DHB plus *N. lutea* proanthocyanidin (blue) in D_2O (Figure S3); ^{1}H NMR spectra of sinapinic acid (red) and of the mixture of sinapinic acid plus *S. bicolor* var. IS8661 proanthocyanidin (blue) in D_2O (Figure S4) (PDF)

https://dx.doi.org/10.1021/acs.jafc.0c04877
J. Agric. Food Chem. 2020, 68, 14038−14048

AUTHOR INFORMATION

Corresponding Author

Ann E. Hagerman − *Department of Chemistry and Biochemistry, Miami University, Oxford, Ohio 45056, United States;* orcid.org/0000-0001-6099-0382; Email: hagermae@miamioh.edu

Authors

Savanah G. Reeves − *Department of Chemistry and Biochemistry, Miami University, Oxford, Ohio 45056, United States*

Arpad Somogyi − *Campus Chemical Instrument Center, Mass Spectrometry and Proteomics Facility, The Ohio State University, Columbus, Ohio 43210, United States*

Wayne E. Zeller − *ARS-USDA, U.S. Dairy Forage Research Center, Madison, Wisconsin 53706, United States;* orcid.org/0000-0002-1883-4519

Theresa A. Ramelot − *Department of Chemistry and Biochemistry, Miami University, Oxford, Ohio 45056, United States*

Kelly C. Wrighton − *Soil & Crop Sciences, Colorado State University, Fort Collins, Colorado 80523, United States*

Complete contact information is available at: https://pubs.acs.org/10.1021/acs.jafc.0c04877

Funding

This work was funded by National Science Foundation, grant number 1750189 to KCW. The 15T Bruker SolariX XR FT-ICR instrument was supported by NIH Award Number Grant S10 OD018507 to the Ohio State University CCIC.

Notes

The authors declare no competing financial interest.

ACKNOWLEDGMENTS

Nuwanthika Kumarage assisted with the proton NMR of DHB adducts and Andre Sommer assisted with the IR instrumentation.

ABBREVIATIONS USED

ATR, attenuated total reflectance; CID, collisional induced dissociation; DHB, 2,5-dihydroxybenzoic acid; DTGS, deuterium triglycine sulfate; EGCg, epigallocatechin gallate; ESI, electrospray ionization; FT-ICR, Fourier transform-ion cyclotron resonance; HCA, α-cyano hydroxycinnamic acid; HPLC−DAD, high performance liquid chromatography−diode array detection; HRF, heterocyclic ring fusion; HSQC, heteronuclear single quantum coherence; IR, infrared; IRE, germanium internal reflection element; MALDI, matrix assisted laser desorption ionization; mDP, mean degree of polymerization; MS, mass spectrometry; NMR, nuclear magnetic resonance; QM, quinone methide; RDA, retro-Diels−Alder; SA, sinapinic acid; TOF, time of flight

REFERENCES

(1) Hagerman, A. E. Fifty years of polyphenol-protein complexes. *Recent Adv. Polyphenol Res.* **2012**, *3*, 71−97.

(2) Santos-Buelga, C.; Scalbert, A. Proanthocyanidins and tannin-like compounds - nature, occurrence, dietary intake and effects on nutrition and health. *J. Sci. Food Agric.* **2000**, *80*, 1094−1117.

(3) Koleckar, V.; Kubikova, K.; Rehakova, Z.; Kuca, K.; Jun, D.; Jahodar, L.; Opletal, L. Condensed and hydrolysable tannins as antioxidants influencing the health. *Mini-Rev. Med. Chem.* **2008**, *8*, 436−447.

(4) Scalbert, A.; Mila, I.; Expert, D.; Marmolle, F.; Albrecht, A.; Hurrell, R.; Huneau, J.; Tome, D. Polyphenols, Metal Ion Complexation and Biological Consequences. In *Plant Polyphenols 2: Chemistry, Biology, Pharmacology, Ecology*; Gross, G. G.; Hemingway, R. W.; Yoshida, R.; Branham, S., Eds.; Kluwer Academic/Plenum Publishers: New York, 1999; pp 545−553.

(5) Constabel, C. P.; Yoshida, K.; Walker, V. Diverse ecological roles of plant tannins: Plant defense and beyond. *Recent Adv. Polyphenol Res.* **2014**, *4*, 115−142.

(6) Serrano, J.; Puupponen-Pimia, R.; Dauer, A.; Aura, A. M.; Saura-Calixto, F. Tannins: Current knowledge of food sources, intake, bioavailability and biological effects. *Mol. Nutr. Food Res.* **2009**, *53*, S310−S329.

(7) Mueller-Harvey, I.; Bee, G.; Dohme-Meier, F.; Hoste, H.; Karonen, M.; Koelliker, R.; Luescher, A.; Niderkorn, V.; Pellikaan, W. F.; Salminen, J.-P.; Skot, L.; Smith, L. M. J.; Thamsborg, S. M.; Totterdell, P.; Wilkinson, I.; Williams, A. R.; Azuhnwi, B. N.; Baert, N.; Brinkhaus, A. G.; Copani, G.; Desrues, O.; Drake, C.; Engstrom, M.; Fryganas, C.; Girard, M.; Huyen, N. T.; Kempf, K.; Malisch, C.; Mora-Ortiz, M.; Quijada, J.; Ramsay, A.; Ropiak, H. M.; Waghorn, G. C. Benefits of condensed tannins in forage legumes fed to ruminants: Importance of structure, concentration, and diet composition. *Crop Sci.* **2019**, *59*, 861−885.

(8) Watrelot, A. A.; Norton, E. L. Chemistry and reactivity of tannins in Vitis spp.: A review. *Molecules* **2020**, *25*, No. 2110.

(9) Cheynier, V. Phenolic compounds: From plants to foods. *Phytochem. Rev.* **2012**, *11*, 153−177.

(10) Sepperer, T.; Tondi, G.; Petutschnigg, A.; Young, T. M.; Steiner, K. Mitigation of ammonia emissions from cattle manure slurry by tannins and tannin-based polymers. *Biomolecules* **2020**, No. 581.

(11) Ishak, N. A. I.; Kamarudin, S. K.; Timmiati, S. N. Green synthesis of metal and metal oxide nanoparticles via plant extracts: An overview. *Mater. Res. Express* **2019**, *6*, No. 112004.

(12) Engström, M. T.; Palijarvi, M.; Fryganas, C.; Grabber, J. H.; Mueller-Harvey, I.; Salminen, J.-P. Rapid qualitative and quantitative analyses of proanthocyanidin oligomers and polymers by UPLC-MS/MS. *J. Agric. Food Chem.* **2014**, *62*, 3390−3399.

(13) Moilanen, J.; Sinkkonen, J.; Salminen, J. P. Characterization of bioactive plant ellagitannins by chromatographic, spectroscopic and mass spectrometric methods. *Chemoecology* **2013**, *23*, 165−179.

(14) Giribaldi, J.; Besson, M.; Suc, L.; Fulcrand, H.; Mouls, L. The use of extracted-ion chromatograms to quantify the composition of condensed tannin subunits. *Rapid Commun. Mass Spectrom.* **2020**, *34*, No. e8619.

(15) Quideau, S.; Deffieux, D.; Douat-Casassus, C.; Pouysegu, L. Plant polyphenols: Chemical properties, biological activities, and synthesis. *Angew. Chem., Int. Ed.* **2011**, *50*, 586−621.

(16) Okuda, T.; Yoshida, T.; Hatano, T.; Ito, H. Ellagitannins Renewed the Concept of Tannins. In *Chemistry and Biology of Ellagitannins: An Underestimated Class of Bioactive Plant Polyphenols*; Quideau, S., Ed.; World Scientific, 2009; pp 1−54.

(17) Yamada, H.; Wakamori, S.; Hirokane, T.; Ikeuchi, K.; Matsumoto, S. Structural revisions in natural ellagitannins. *Molecules* **2018**, *23*, No. 1901.

(18) Leppä, M. M.; Karonen, M.; Tahtinen, P.; Engstrom, M. T.; Salminen, J. P. Isolation of chemically well-defined semipreparative liquid chromatography fractions from complex mixtures of proanthocyanidin oligomers and polymers. *J. Chromatogr. A* **2018**, *1576*, 67−79.

(19) Scioneaux, A. N.; Schmidt, M. A.; Moore, M. A.; Lindroth, R. L.; Wooley, S. C.; Hagerman, A. E. Qualitative variation in proanthocyanidin composition of Populus species and hybrids: Genetics is the key. *J. Chem. Ecol.* **2011**, *37*, 57−70.

(20) Li, C.; Leverence, R.; Trombley, J. D.; Xu, S.; Yang, J.; Tian, Y.; Reed, J. D.; Hagerman, A. E. High molecular weight persimmon (Diospyros kaki L.) proanthocyanidin: A highly galloylated, a-linked tannin with an unusual flavonol terminal unit, myricetin. *J. Agric. Food Chem.* **2010**, *58*, 9033−9042.

(21) Karonen, M.; Loponen, J.; Ossipov, V.; Pihlaja, K. Analysis of procyanidins in pine bark with reversed-phase and normal-phase high-performance liquid chromatography-electrospray ionization mass spectrometry. *Anal. Chim. Acta* **2004**, *522*, 105−112.
(22) Rush, M. D.; Rue, E. A.; Wong, A.; Kowalski, P.; Glinsk, J. A.; van Breemen, R. B. Rapid determination of procyanidins using MALDI-TOF/TOF mass spectrometry. *J. Agric. Food Chem.* **2018**, *66*, 11355−11361.
(23) Krueger, C. G.; Vestling, M. M.; Reed, J. D. Matrix-assisted laser desorption/ionization time-of-flight mass spectrometry of heteropolyflavan-3-ols and glucosylated heteropolyflavans in sorghum [*S. bicolor* (L.) Moench]. *J. Agric. Food Chem.* **2003**, *51*, 538−543.
(24) Neilson, A. P.; O'Keefe, S. F.; Bolling, B. W. High-molecular-weight proanthocyanidins in foods: Overcoming analytical challenges in pursuit of novel dietary bioactive components. *Annu. Rev. Food Sci. Technol.* **2016**, *7*, 43−64.
(25) Zeller, W. E. Activity, purification, and analysis of condensed tannins: Current state of affairs and future endeavors. *Crop Sci.* **2019**, *59*, 886−904.
(26) Rue, E. A.; Rush, M. D.; van Breemen, R. B. Procyanidins: A comprehensive review encompassing structure elucidation via mass spectrometry. *Phytochem. Rev.* **2018**, *17*, 1−16.
(27) Naumann, H.; Sepela, R.; Rezaire, A.; Masih, S. E.; Zeller, W. E.; Reinhardt, L. A.; Robe, J. T.; Sullivan, M. L.; Hagerman, A. E. Relationships between structures of condensed tannins from Texas legumes and methane production during in vitro rumen digestion. *Molecules* **2018**, 23.
(28) Feliciano, R. P.; Shea, M. P.; Shanmuganayagam, D.; Krueger, C. G.; Howell, A. B.; Reed, J. D. Comparison of isolated cranberry (Vaccinium macrocarpon Ait.) proanthocyanidins to catechin and procyanidins A2 and B2 for use as standards in the 4-(dimethylamino)cinnamaldehyde assay. *J. Agric. Food Chem.* **2012**, *60*, 4578−4585.
(29) Hurst, W. J.; Stanley, B.; Glinski, J. A.; Davey, M.; Payne, M. J.; Stuart, D. A. Characterization of primary standards for use in the HPLC analysis of the procyanidin content of cocoa and chocolate containing products. *Molecules* **2009**, *14*, 4136−4146.
(30) Jiang, Y.; Zhang, H.; Qi, X.; Wu, G. Structural characterization and antioxidant activity of condensed tannins fractionated from Sorghum grain. *J. Cereal Sci.* **2020**, *92*, No. 102918.
(31) Gupta, R. K.; Haslam, E. Plant proanthocyanidins. Part 5. Sorghum polyphenols. *J. Chem. Soc., Perkin Trans. 1* **1978**, *1978*, 892−896.
(32) Hagerman, A. E.; Butler, L. G. Condensed tannin purification and characterization of tannin-associated proteins. *J. Agric. Food Chem.* **1980**, *28*, 947−952.
(33) Hagerman, A. E. Tannin Handbook, 2011. http://www.Users.Miamioh.Edu/hagermae/.
(34) Naumann, H. D.; Hagerman, A. E.; Lambert, B. D.; Muir, J. P.; Tedeschi, L. O.; Kothmann, M. M. Molecular weight and protein-precipitating ability of condensed tannins from warm-season perennial legumes. *J. Plant Interact.* **2014**, *9*, 212−219.
(35) Roullier-Gall, C.; Witting, M.; Gougeon, R. D.; Schmitt-Kopplin, P. High precision mass measurements for wine metabolomics. *Front. Chem.* **2014**, *2*, No. 102.
(36) Laszakovits, J. R.; Somogyi, A.; MacKay, A. A. Chemical alterations of dissolved organic matter by permanganate oxidation. *Environ. Sci. Technol.* **2020**, *54*, 3256−3266.
(37) Zhang, M.; Sun, J.; Chen, P. A computational tool for accelerated analysis of oligomeric proanthocyanidins in plants. *J. Food Comput. Anal.* **2017**, *56*, 124−133.
(38) Cooper, K. A.; Campos-Gimenez, E.; Alvarez, D. J.; Nagy, K.; Donovan, J. L.; Williamson, G. Rapid reversed phase ultra-performance liquid chromatography analysis of the major cocoa polyphenols and inter-relationships of their concentrations in chocolate. *J. Agric. Food Chem.* **2007**, *55*, 2841−2847.
(39) Zeller, W. E.; Ramsay, A.; Ropiak, H. M.; Fryganas, C.; Mueller-Harvey, I.; Brown, R. H.; Drake, C.; Grabber, J. H. H-1-C-13 HSQC NMR spectroscopy for estimating procyanidin/prodelphinidin and *cis*/*trans*-flavan-3-ol ratios of condensed tannin samples: Correlation with thiolysis. *J. Agric. Food Chem.* **2015**, *63*, 1967−1973.
(40) Ölschläger, C.; Regos, I.; Zeller, F. J.; Treutter, D. Identification of galloylated propelargonidins and procyanidins in buckwheat grain and quantification of rutin and flavanols from homostylous hybrids originating from F esculentum x F homotropicum. *Phytochemistry* **2008**, *69*, 1389−1397.
(41) Macha, S. F.; Limbach, P. A. Matrix-assisted laser desorption/ionization (MALDI) mass spectrometry of polymers. *Curr. Opin. Solid State Mater. Sci.* **2002**, *6*, 213−220.
(42) Lin, L.-Z.; Sun, J.; Chen, P.; Monagas, M. J.; Harnly, J. M. UHPLC-PDA-ESUHRMSN profiling method to identify and quantify oligomeric proanthocyanidins in plant products. *J. Agric. Food Chem.* **2014**, *62*, 9387−9400.
(43) Esquivel-Alvarado, D.; Alfaro-Viquez, E.; Krueger, C. G.; Vestling, M. M.; Reed, J. D. Classification of proanthocyanidin profiles using matrix-assisted laser desorption/ionization time-of-flight mass spectrometry (MALDI-TOF MS) spectra data combined with multivariate analysis. *Food Chem.* **2020**, *336*, 127667.
(44) Dixon, R. A.; Xie, D.-Y.; Sharma, S. B. Proanthocyanidins a final frontier in flavonoid research? *New Phytol.* **2005**, *165*, 9−28.
(45) Osman, A. M.; Wong, K. K. Y. Laccase (EC 1.10.3.2) catalyses the conversion of procyanidin B-2 (epicatechin dimer) to type A-2. *Tetrahedron Lett.* **2007**, *48*, 1163−1167.
(46) Chen, L.; Yuan, P.; Chen, K.; Jia, Q.; Li, Y. Oxidative conversion of B- to A-type procyanidin trimer: Evidence for quinone methide mechanism. *Food Chem.* **2014**, *154*, 315−322.
(47) Liu, H.; Howell, A. B.; Zhang, D. J.; Khoo, C. A randomized, double-blind, placebo-controlled pilot study to assess bacterial anti-adhesive activity in human urine following consumption of a cranberry supplement. *Food Funct.* **2019**, *10*, 7645−7652.
(48) Spencer, P.; Sivakumaran, S.; Fraser, K.; Foo, L. Y.; Lane, G. A.; Edwards, P. J. B.; Meagher, L. P. Isolation and characterisation of procyanidins from Rumex obtusifolius. *Phytochem. Anal.* **2007**, *18*, 193−203.
(49) Cai, Y.; Gaffney, S. H.; Lilley, T. H.; Magnolato, D.; Martin, R.; Spencer, C. M.; Haslam, E. Polyphenol interactions. Part 4. Model studies with caffeine and cyclodextrins. *J. Chem. Soc., Perkin Trans. 2* **1990**, 2197−2209.
(50) Schneider, H. J. Binding mechanisms in supramolecular complexes. *Angew. Chem., Int. Ed.* **2009**, *48*, 3924−3977.
(51) Trouillas, P.; Sancho-Garcia, J. C.; De Freitas, V.; Gierschner, J.; Otyepka, M.; Dangles, O. Stabilizing and modulating color by copigmentation: Insights from review theory and experiment. *Chem. Rev.* **2016**, *116*, 4937−4982.
(52) Mistry, T. V.; Cai, Y.; Lilley, T. H.; Haslam, E. Polyphenol interactions. Part 5. Anthocyanin copigmentation. *J. Chem. Soc., Perkin Trans. 2* **1991**, *1991*, 1287−1296.
(53) Nave, F.; Bras, N. F.; Cruz, L.; Teixeira, N.; Mateus, N.; Ramos, M. J.; Di Meo, F.; Trouillas, P.; Dangles, O.; De Freitas, V. Influence of a flavan-3-ol substituent on the affinity of anthocyanins (pigments) toward vinylcatechin dimers and proanthocyanidins (copigments). *J. Phys. Chem. B* **2012**, *116*, 14089−14099.
(54) Liu, C.; Li, M.; Yang, J.; Xiong, L.; Sun, Q. Fabrication and characterization of biocompatible hybrid nanoparticles from spontaneous co-assembly of casein/gliadin and proanthocyanidin. *Food Hydrocolloids* **2017**, *73*, 74−89.
(55) Mele, A.; Malpezzi, L. Noncovalent association phenomena of 2,5-dihydroxybenzoic acid with cyclic and linear oligosaccharides. A matrix-assisted laser desorption/ionization time-of-flight mass spectrometric and X-ray crystallographic study. *J. Am. Soc. Mass Spectrom.* **2000**, *11*, 228−236.
(56) Monagas, M.; Quintanilla-Lopez, J. E.; Gomez-Cordoves, C.; Bartolome, B.; Lebron-Aguilar, R. MALDI-TOF MS analysis of plant proanthocyanidins. *J. Pharm. Biomed. Anal.* **2010**, *51*, 358−372.
(57) Dangles, O.; Brouillard, R. A spectroscopic method based on the anthocyanin copigmentation interaction and applied to the quantitative study of molecular-complexes. *J. Chem. Soc., Perkin Trans. 2* **1992**, *1992*, 247−257.

https://dx.doi.org/10.1021/acs.jafc.0c04877
J. Agric. Food Chem. 2020, 68, 14038−14048

(58) Pizzi, A.; Pasch, H.; Rode, K.; Giovando, S. Polymer structure of commercial hydrolyzable tannins by matrix-assisted laser desorption/ionization-time-of-flight mass spectrometry. *J. Appl. Polym. Sci.* **2009**, *113*, 3847−3859.

https://dx.doi.org/10.1021/acs.jafc.0c04877
J. Agric. Food Chem. 2020, 68, 14038−14048